

A Physically Based Approach in Retrieving Vegetation Leaf Area Index from Landsat Surface Reflectance Data

Sangram Ganguly, NASA ARC / BAERI

Ramakrishna Nemani, NASA ARC

Weile Wang, CSU Monterey Bay

Hirofumi Hashimoto, CSU Monterey Bay

Petr Votava, CSU Monterey Bay

Andy Michaelis, CSU Monterey Bay

Cristina Milesi, CSU Monterey Bay

Forrest S. Melton, NASA ARC

Jennifer Dungan, NASA ARC

Ranga B. Myneni, Boston University

Leaf Area Index Heritage

- Robust theoretical approaches exist in the MODIS LAI retrieval algorithm;
- Spectral invariant theory based on the 3D stochastic radiative transfer model has been developed – a very efficient way to simulate the realistic model that generates BRF (Bidirectional Reflectance Factor) as a function of LAI, soil reflectances and view/azimuth angles;
- Theoretical understanding in place to account for variations in spatial resolution and spectral bandwidth between sensors in LAI retrieval;
- Spectral reflectance or NDVI based inversion methods to generate LAI are always preferred as they are not based on heuristics. NDVI-LAI empirical relationships are not encouraged as they are region specific and functional relationships can change dramatically.

Surface Reflectances Process Overview

- Global Land Survey (GLS) datasets are obtained from EDC DAAC;
- Processing of GLS scenes using LEDAPS from GSFC for radiometric calibration and atmospheric corrections to derive first-pass surface reflectances (SRs);
- MODIS Collection 5 Landcover map downscaled to 30m as an initial input to LAI estimation;
- For continental US, 30-m NLCD landcover map is also used as input to LAI estimation.
- MODIS Collection 5 (MCD43A4) NBAR surface reflectance product utilized for testing reflectance consistency.

Spectral Invariants: Parameterization of Spectral Reflectance

- Radiative transfer theory of canopy spectral invariants provides the required Bidirectional Reflectance Function (BRF) parameterization via a small set of well defined measured variables;
- These variables specify the relationship between the spectral response of a scattering object bounded by a non-reflecting surface to the incident radiation at different spatial scales;
- Spectral invariant form of BRF can decouple the **structural and spectral information**.

$$BRF_{\lambda} = \omega_{\lambda}R_1 + \frac{\omega_{\lambda}^2R_2}{1 - p\omega_{\lambda}}$$

Spectral Information

Structural information

R_1, R_2 : Escape probabilities

p : Recollision probability

ω_{λ} : Single scattering albedo

Stochastic RT Model & Spectral Invariants

The three-dimensional radiative transfer problem with arbitrary boundary conditions can be expressed as a superposition of some basic radiative transfer sub-problems with purely absorbing boundaries and to which the notion of spectral invariant can be directly applied

$$\begin{array}{l}
 \text{Spectral invariant form} \quad \text{BRF}_{\text{BS},\lambda}(\Omega) = \omega_\lambda R_1(\Omega) + \frac{\omega_\lambda^2}{1-p\omega_\lambda} R_2(\Omega) \quad \left| \quad \begin{array}{l} t_{\text{BS},\lambda}(\Omega) = t_0 + \omega_\lambda T_1(\Omega) + \frac{\omega_\lambda^2 T_2(\Omega)}{1-p_t\omega_\lambda} \\ J_{S,\lambda}(\Omega) = J_0 + \omega_\lambda J_1(\Omega) + \frac{\omega_\lambda^2 J_2(\Omega)}{1-p_j\omega_\lambda} \end{array} \\
 \\
 \text{3D RT form} \quad \text{BRF}_\lambda(\Omega) = \text{BRF}_{\text{BS},\lambda}(\Omega) + \frac{\rho_{\text{sur},\lambda}}{1-\rho_{\text{sur},\lambda}r_{S,\lambda}} t_{\text{BS},\lambda} J_{S,\lambda}(\Omega) \quad \left| \quad a_\lambda = a_{\text{BS},\lambda} + \frac{\rho_{\text{sur},\lambda}}{1-\rho_{\text{sur},\lambda}r_{S,\lambda}} t_{\text{BS},\lambda} a_{S,\lambda}
 \end{array}$$

$J_{(s,\lambda)}$ – radiance generated by isotropic sources ($1/\pi$) at the canopy bottom.

Taking into account the intensity of sources at the first interaction is

$(1/\pi) * t_{(\text{BS},\lambda)} * \rho_{(\text{sur},\lambda)}$, corresponding radiance from surface can be expressed as

$J_{(s,\lambda)} * t_{(\text{BS},\lambda)} * \rho_{(\text{sur},\lambda)}$. Total radiance “S” can be expressed as successive orders of scattering,

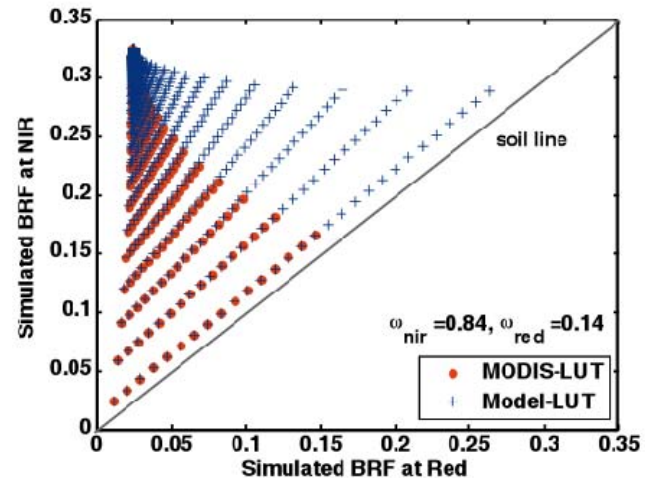
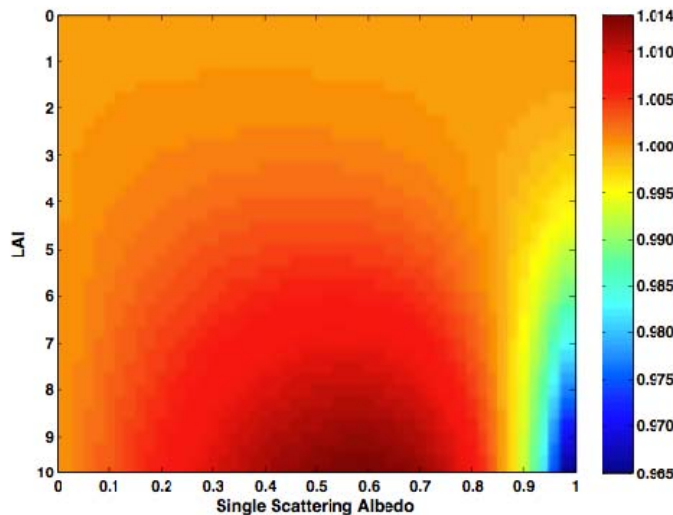
$$\begin{aligned}
 S &= t_{\text{BS},\lambda} \rho_{\text{sur},\lambda} J_{S,\lambda}(\Omega) + \rho_{\text{sur},\lambda}^2 r_{S,\lambda} t_{\text{BS},\lambda} J_{S,\lambda}(\Omega) + \rho_{\text{sur},\lambda}^3 r_{S,\lambda}^2 t_{\text{BS},\lambda} J_{S,\lambda}(\Omega) + \dots \\
 &\quad + \rho_{\text{sur},\lambda}^n r_{S,\lambda}^{n-1} t_{\text{BS},\lambda} J_{S,\lambda}(\Omega),
 \end{aligned}$$

$$S = \frac{\rho_{\text{sur},\lambda}}{1-\rho_{\text{sur},\lambda}r_{S,\lambda}} t_{\text{BS},\lambda} J_{S,\lambda}(\Omega)$$

Spectral Invariant Approximation

The total problem can be solved using the spectral invariant approximation

$$BRF_{\lambda}(\Omega) = \left\{ \omega_{\lambda} R_1(\Omega) + \frac{\omega_{\lambda}^2}{1-p\omega_{\lambda}} R_2(\Omega) \right\} + \left\{ \begin{aligned} &\rho_{sur,\lambda} \times \left[t_0 + \omega_{\lambda} T_1(\Omega) + \frac{\omega_{\lambda}^2 T_2(\Omega)}{1-p_t \omega_{\lambda}} \right] \times \left[J_0 + \omega_{\lambda} J_1(\Omega) + \frac{\omega_{\lambda}^2 J_2(\Omega)}{1-p_j \omega_{\lambda}} \right] \\ &1 - \rho_{sur,\lambda} \times \left[\omega_{\lambda} \bar{R}_{1,S} + \frac{\omega_{\lambda}^2 \bar{R}_{2,S}}{1-p_{r,S} \omega_{\lambda}} \right] \end{aligned} \right\}$$



Biome specific LUTs can be efficiently created using the relation above

Adjustment for Spectral/Spatial Resolution

$$\frac{\int_{\lambda_1}^{\lambda_2} BRF(\lambda) \times f_{sr}(\lambda) d\lambda}{\int_{\lambda_1}^{\lambda_2} f_{sr}(\lambda) d\lambda} = R_1 \frac{\int_{\lambda_1}^{\lambda_2} \omega(\lambda) \times f_{sr}(\lambda) d\lambda}{\int_{\lambda_1}^{\lambda_2} f_{sr}(\lambda) d\lambda} + R_2 \frac{\int_{\lambda_1}^{\lambda_2} \frac{\omega(\lambda)^2}{1 - p\omega(\lambda)} \times f_{sr}(\lambda) d\lambda}{\int_{\lambda_1}^{\lambda_2} f_{sr}(\lambda) d\lambda}$$

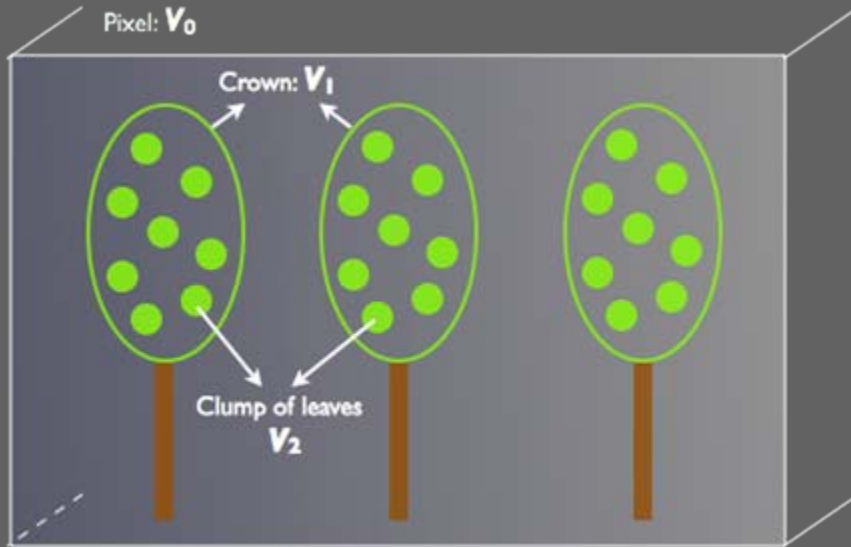
Ratio

$$\overline{BRF} = R_1 \overline{\omega} + R_2 \frac{\overline{\omega^2}}{1 - p\overline{\omega}} \left(\frac{\int_{\lambda_1}^{\lambda_2} \frac{\omega(\lambda)^2}{1 - p\omega(\lambda)} \times f_{sr}(\lambda) d\lambda}{\int_{\lambda_1}^{\lambda_2} f_{sr}(\lambda) d\lambda \times \frac{\overline{\omega^2}}{1 - p\overline{\omega}}} \right)$$

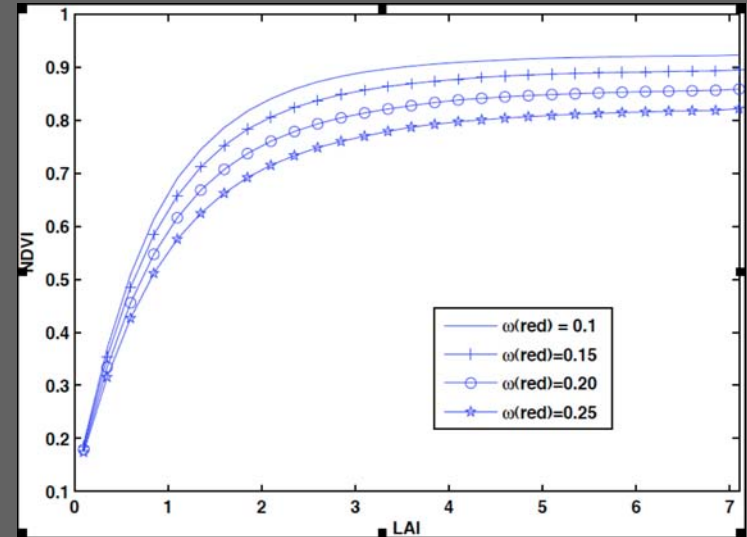
Integrate the “Ratio” for two different bandwidths corresponding to the red (580-680 nm) and NIR (725-1100 nm) bands.

Approximation to unity suggest the fact that differences in spectral characteristics between sensors can be solved by averaging the single scattering albedo over the sensor bandwidths

Adjustment for Spatial Resolution

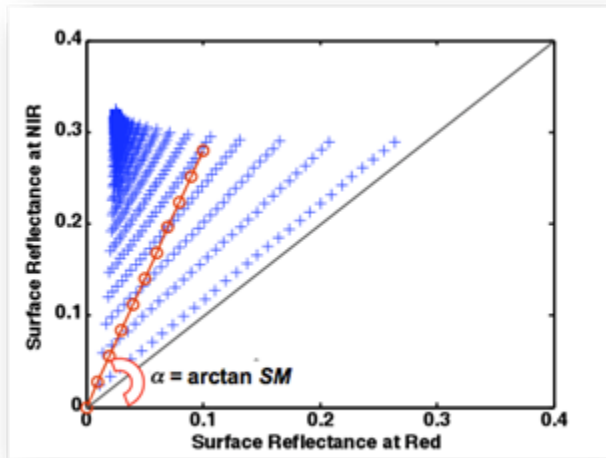


$$\omega_\lambda(V_1) = \omega_\lambda(V_2) \frac{1 - p(V_2 \rightarrow V_1)}{1 - \omega_\lambda(V_2) \cdot p(V_2 \rightarrow V_1)}$$



LAI-NDVI relationships for different values of single scattering albedo

LAI Inversion Methodology



Each pixel can have a background ranging from dark soil to bright soils, and the LAI can vary over a range for each specific instance of background brightness

- The following merit function is used to generate acceptable solutions in the **Inversion-mode**:

$$\Delta^2 = \frac{(NIR^* - NIR)^2}{\sigma_{NIR}^2} + \frac{(red^* - red)^2}{\sigma_{red}^2}$$

Here $NIR^*(NIR)$ and $red^*(red)$ are the Landsat-measured (RT simulated) surface reflectances respectively.

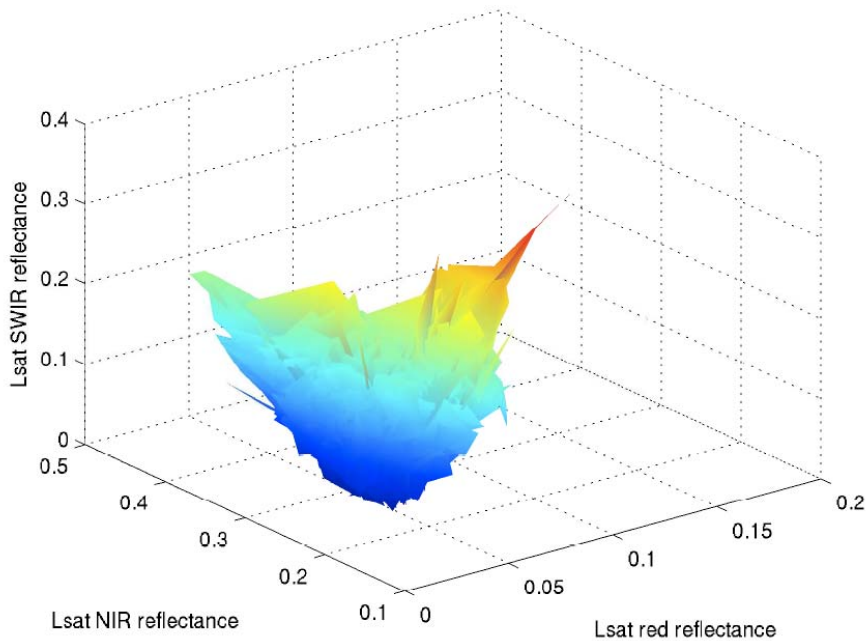
$$\sigma_{NIR} = \epsilon_{NIR} \cdot NIR^*$$

$$\sigma_{red} = \epsilon_{red} \cdot red^*$$

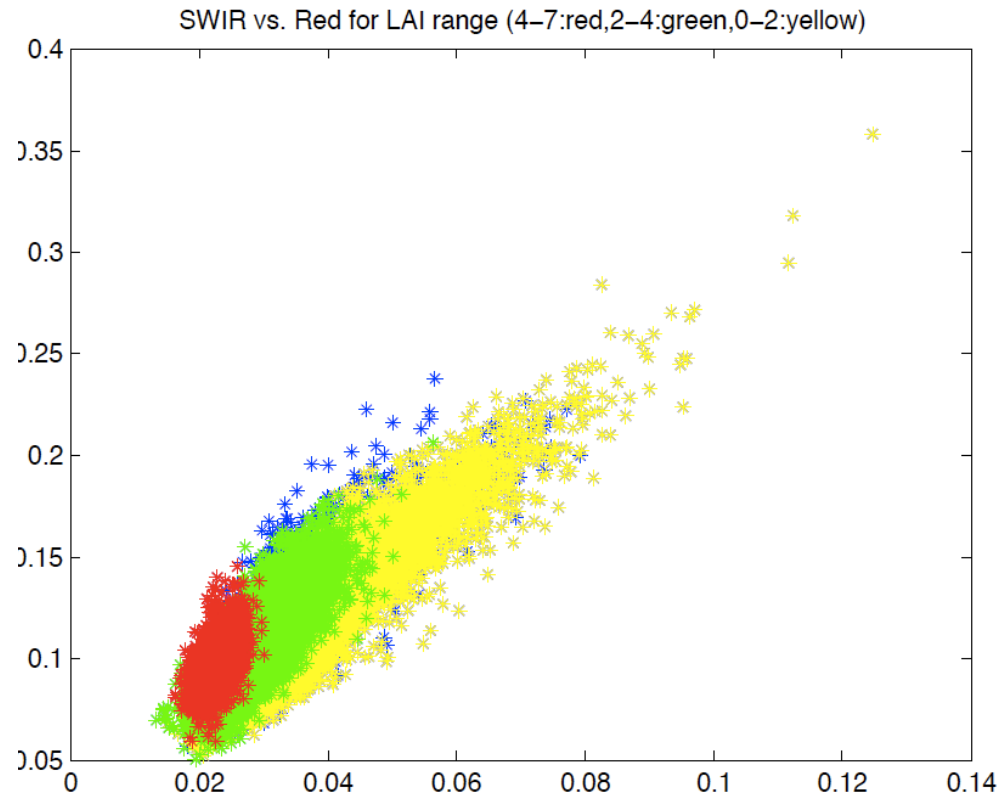
ϵ_{NIR} and ϵ_{red} are corresponding relative uncertainties in measured surface reflectances in NIR and red bands

A value of $\Delta^2 \leq 2$ indicates good proximity between observations and simulations

Reflectance Characterization at Landsat Scale



Reflectance characterization in the Red, NIR and SWIR plane



SWIR vs. Red scatter plot for different LAI ranges (y-axis: SWIR; x-axis: Red).

NDVI vs. Retrieved LAI (2-band vs. 3-band)

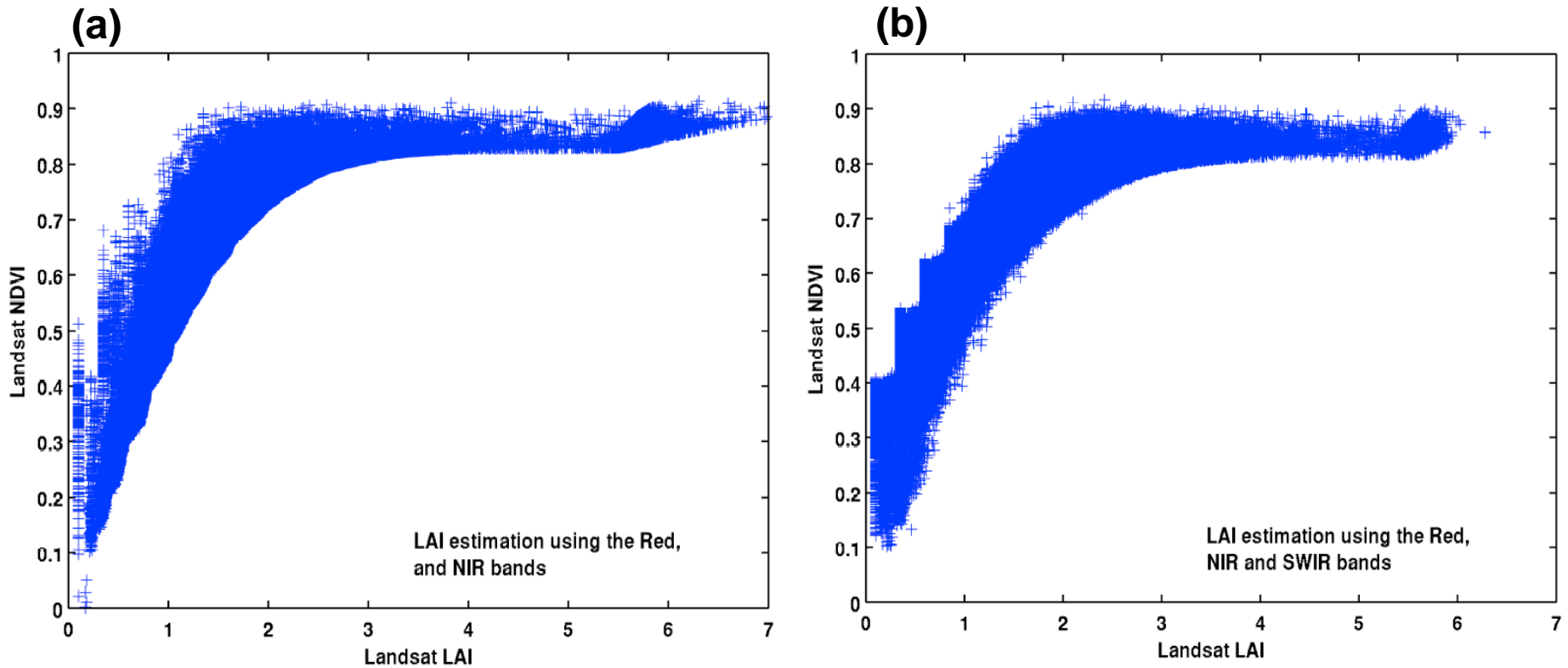


Figure 1. a) Landsat NDVI vs. Landsat retrieved LAI using 2-band only for needleleaf forests. (b) Same as (a) but using a 3-band retrieval scheme. (all needleleaf pixels from Fig. 2 are used)

Landsat vs. MODIS LAI

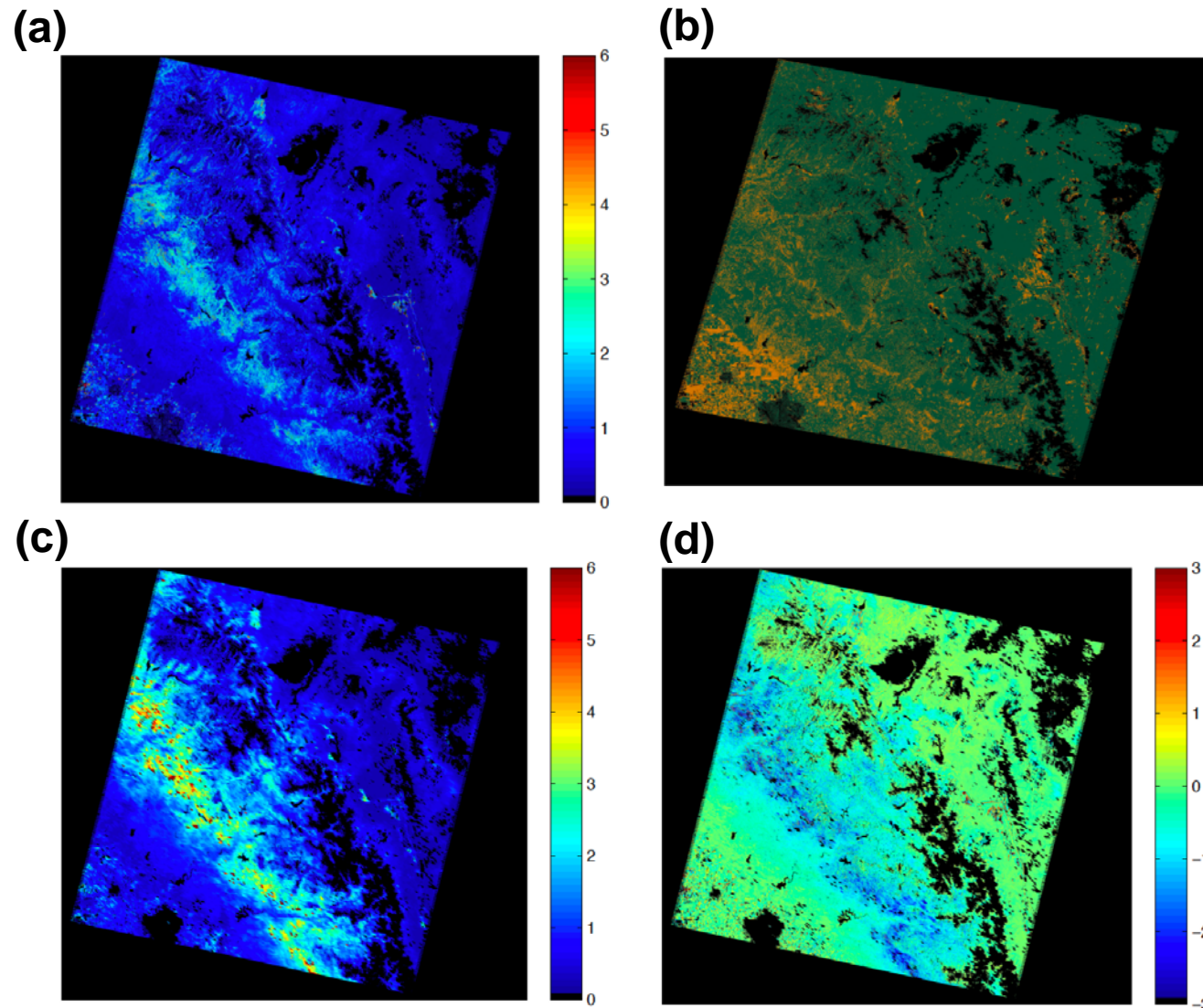
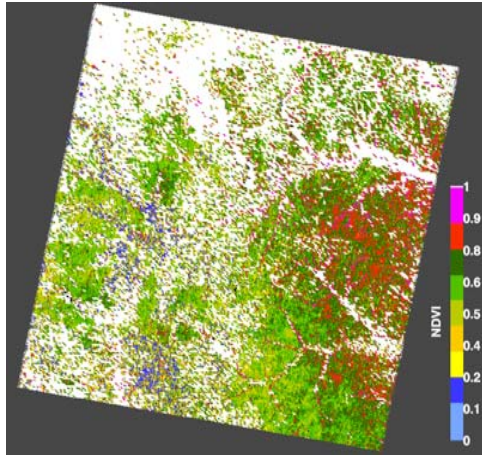


Figure 2. (a) Landsat derived 30-m LAI map using the 3-band and 2-band retrieval scheme. (b) Landsat Quality layer displaying pixels that are retrieved using 3-band (green in color) and 2-band (yellow in color) (c) MODIS 1Km LAI map resampled to 30-m. (d) LAI difference map (Landsat – MODIS).

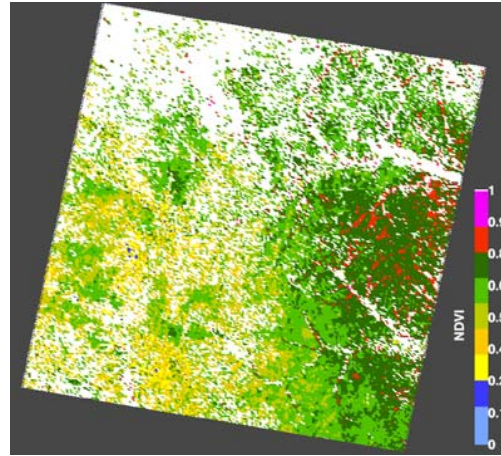
Northern California
Landsat Tile

Analysis at 30-m (Surface Reflectance and LAI)

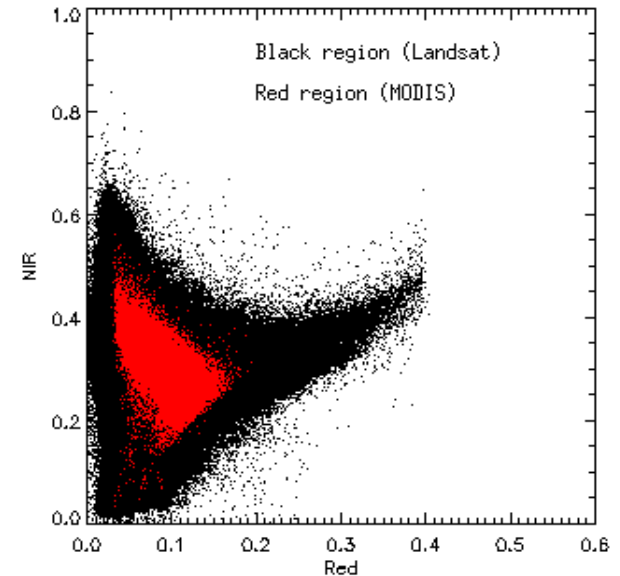
Kansas Prairie (grasslands): Acquisition – 23rd July



Landsat NDVI

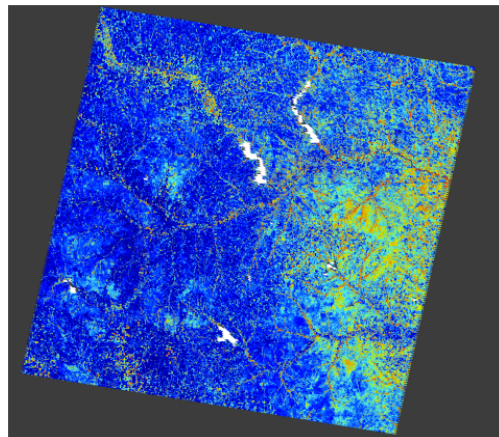


MODIS NDVI

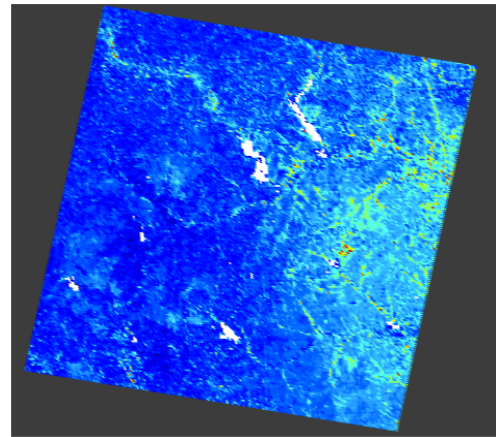


Landsat & MODIS Red/NIR
scatter plot for grassland pixels

LAI derived based on NDVI/ SR



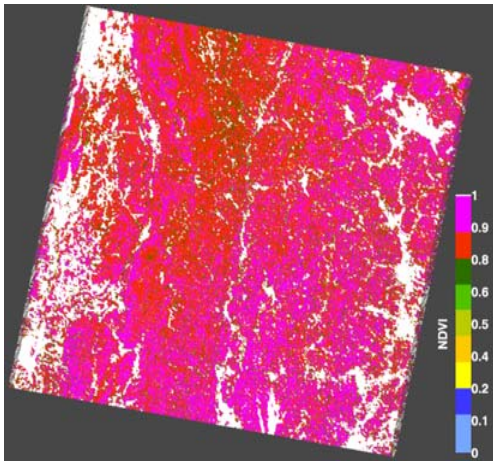
Landsat LAI



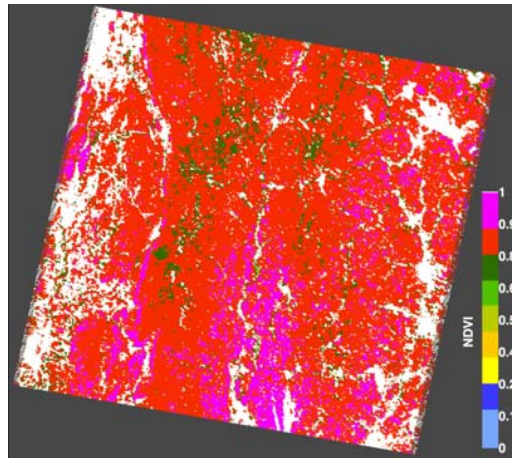
MODIS LAI

Analysis at 30-m (Surface Reflectance and LAI)

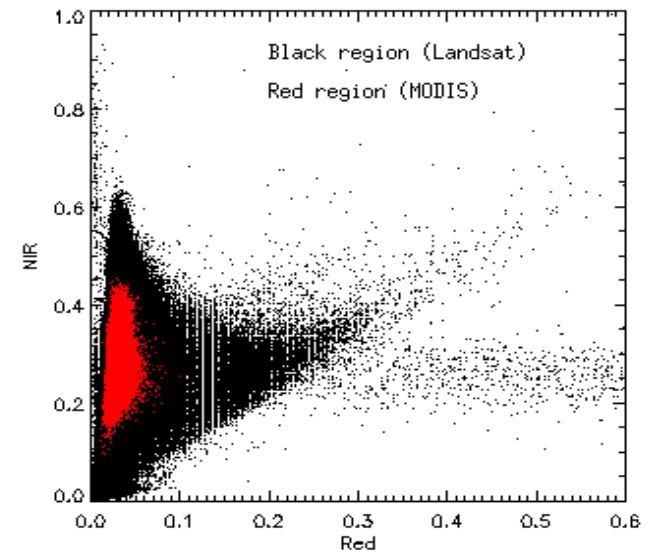
Harvard Forest (B.D.F): Acquisition – 24th September



Landsat NDVI

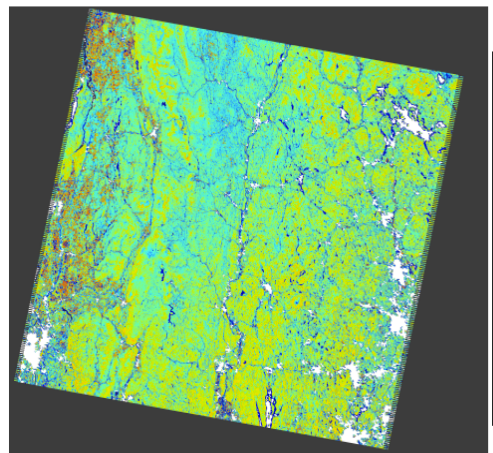


MODIS NDVI

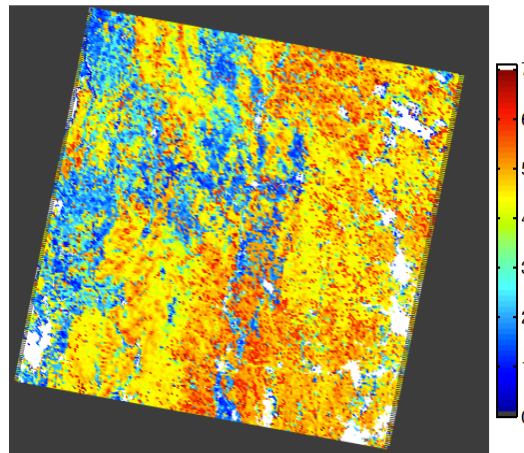


Landsat & MODIS Red/NIR
scatter plot for B.D.F pixels

LAI derived based on NDVI/ SR

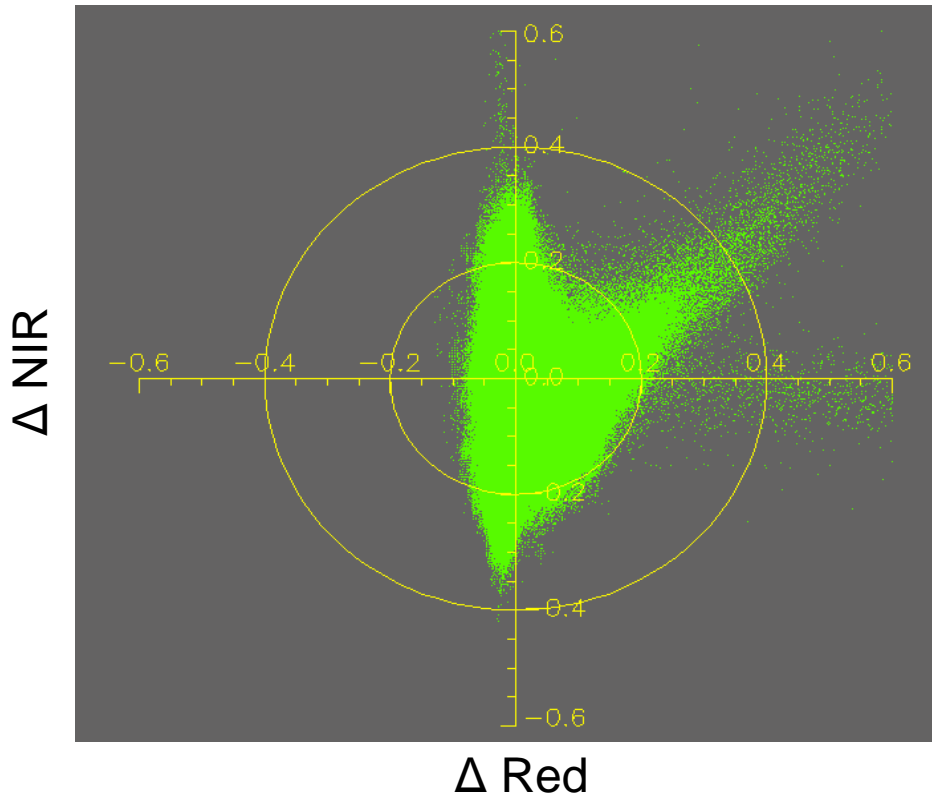


Landsat LAI



MODIS LAI

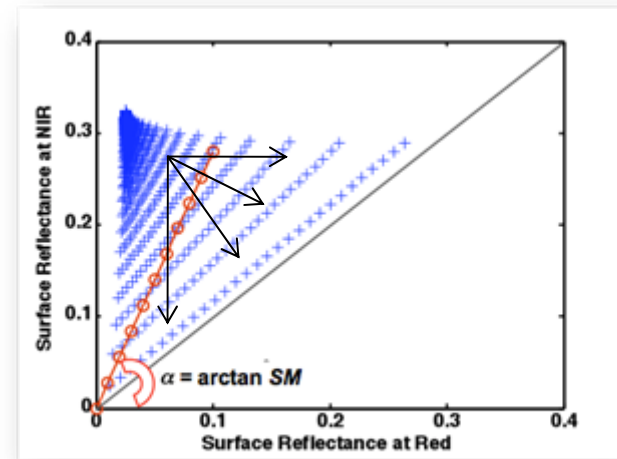
Lower LAI ? – What's the reason



Polar plot showing the direction and magnitude of reflectance differences for all B.D.F pixels

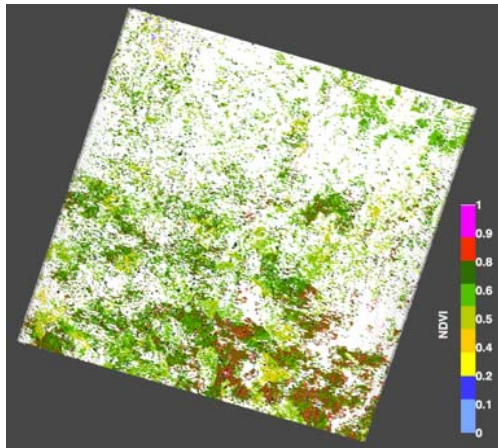
$$\Delta = \text{Landsat} - \text{MODIS}$$

Direction $\{\tan^{-1}(\Delta \text{NIR}/\Delta \text{red})\}$ of pixel differences in majority lies below the 45 degree angle – hits the lower LAI isoline

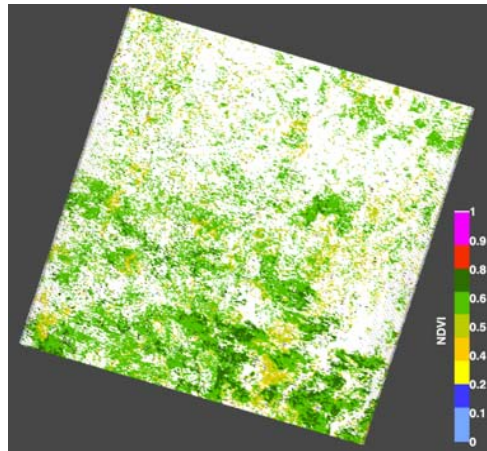


Analysis at 30-m (Surface Reflectance and LAI)

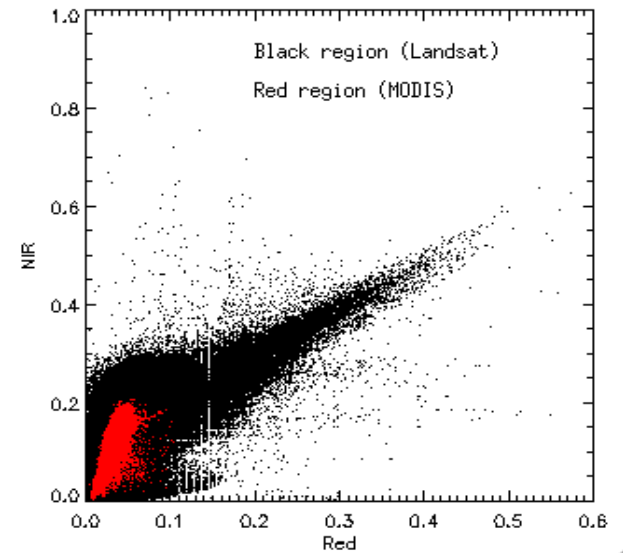
Canada (Boreas - needleleaf): Acquisition – 24th September



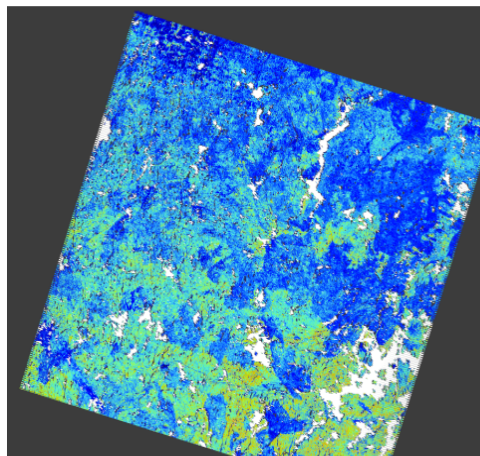
Landsat NDVI



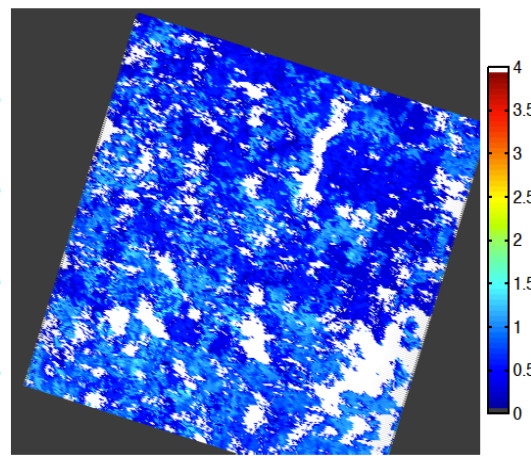
MODIS NDVI



Landsat & MODIS Red/NIR scatter plot for B.D.F pixels



Landsat LAI

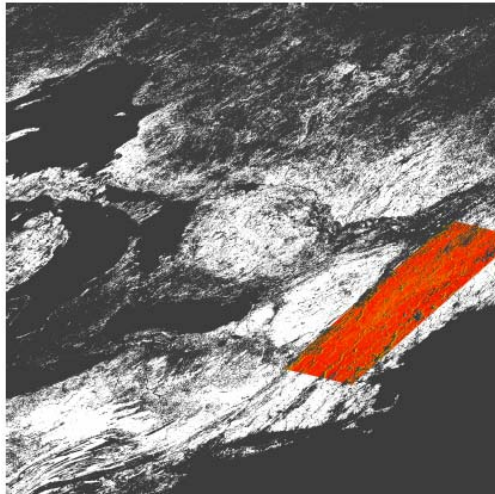


MODIS LAI

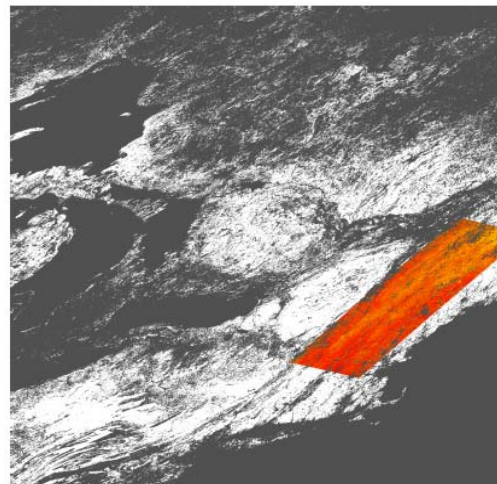
LAI derived based on NDVI/ SR

Analysis at 500-m (Surface Reflectance and LAI)

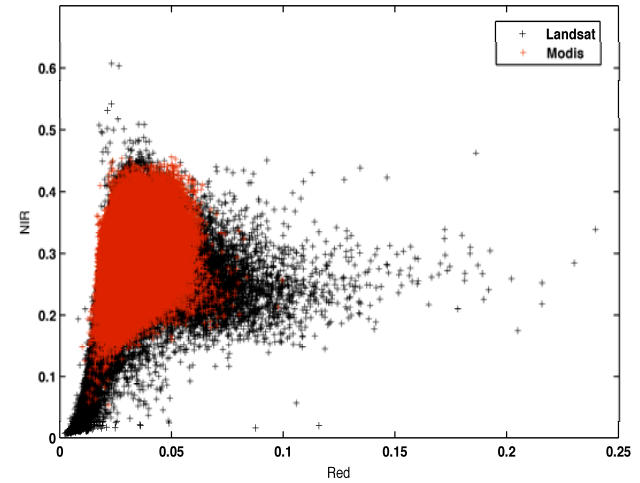
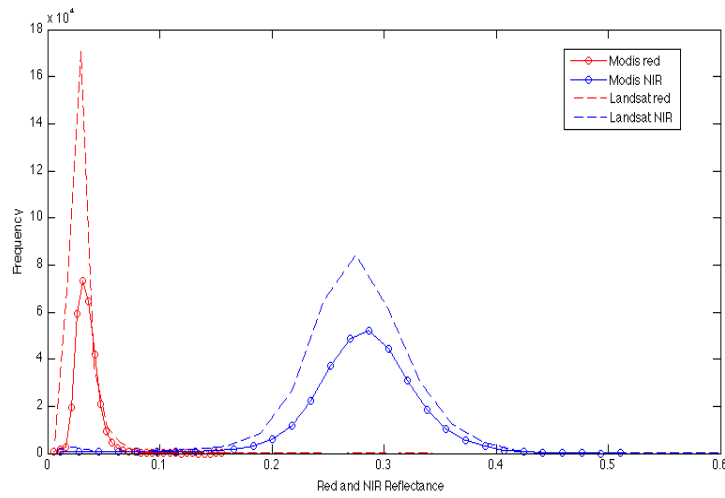
Harvard Forest (B.D.F): Acquisition – 24th September



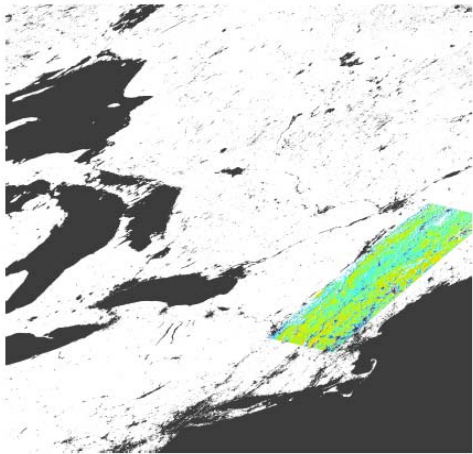
Landsat NDVI



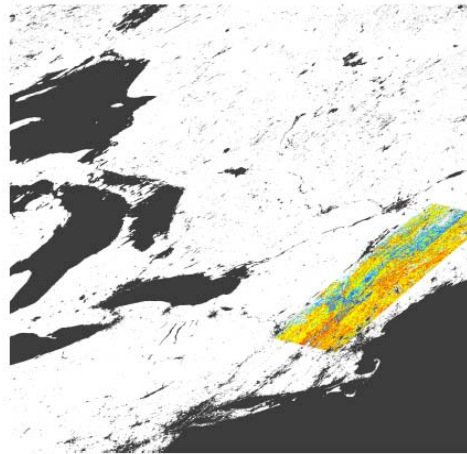
MODIS NDVI



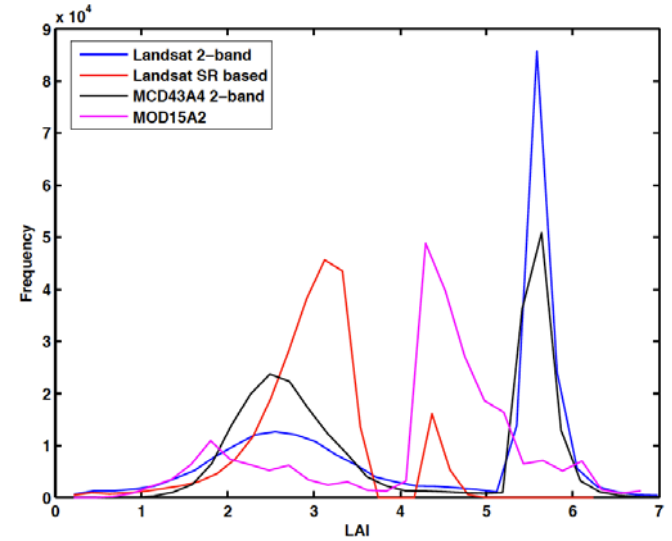
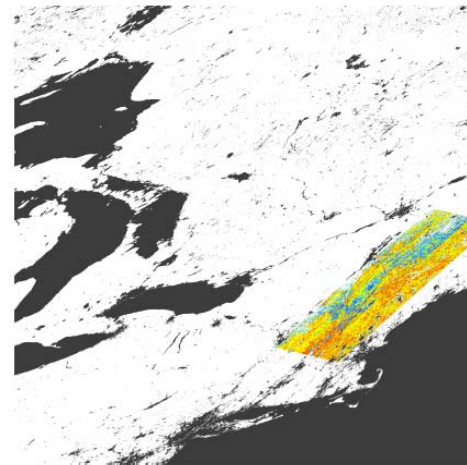
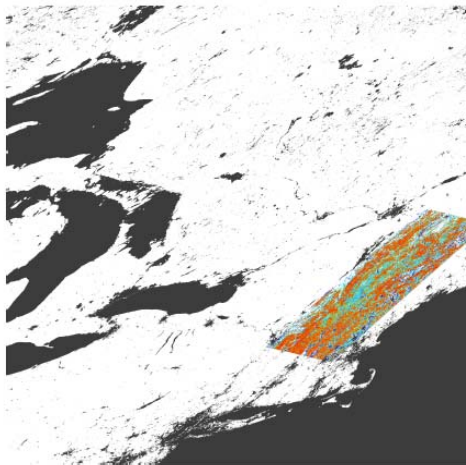
Analysis at 500-m (Surface Reflectance and LAI)



Landsat LAI

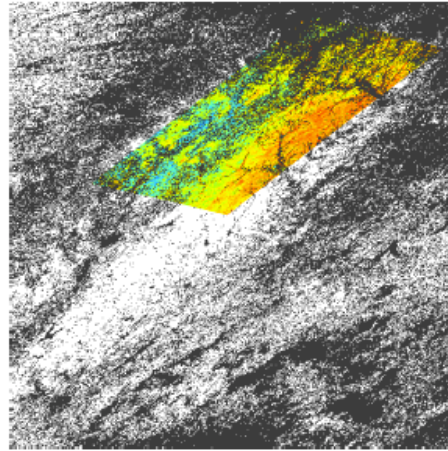
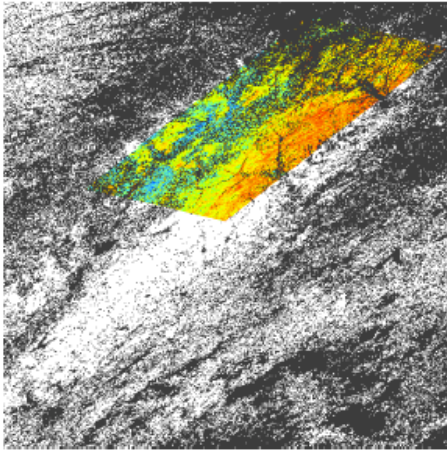


MODIS LAI



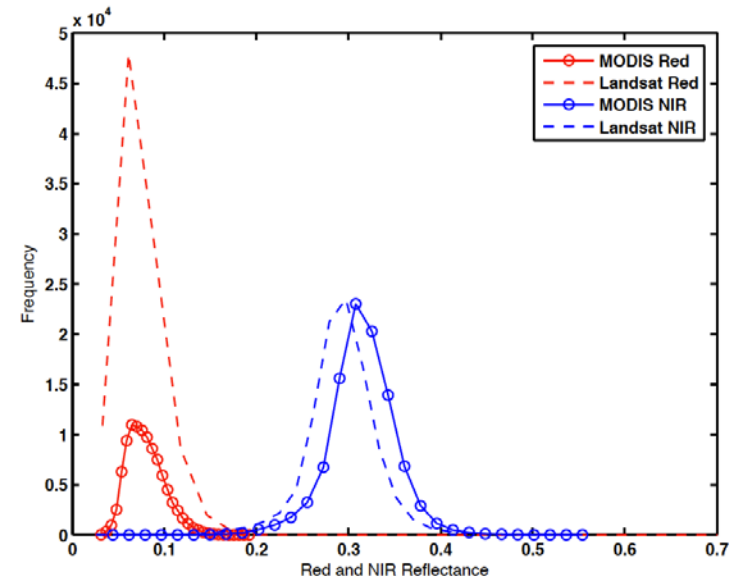
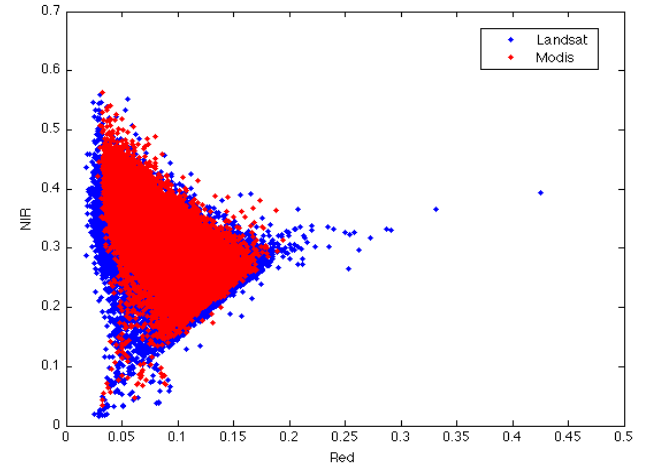
Analysis at 500-m (Surface Reflectance and LAI)

Kansas Cropland/grassland : Acquisition – 23rd July



Landsat NDVI

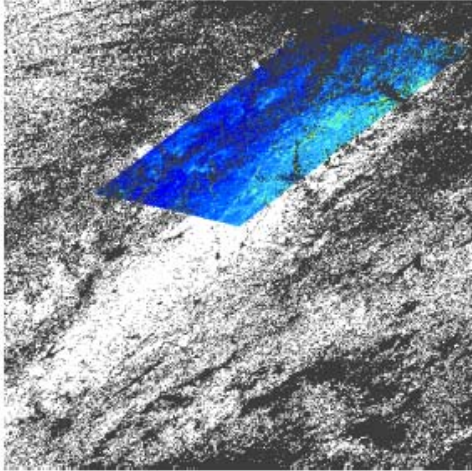
MODIS NDVI



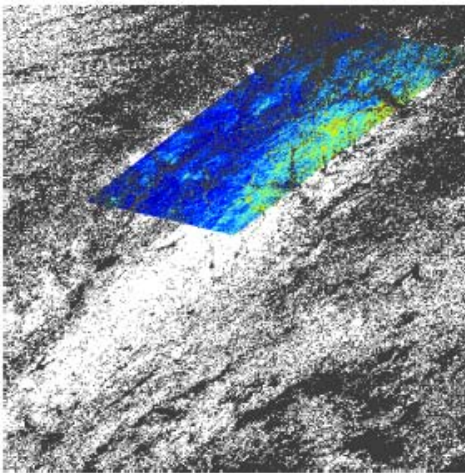
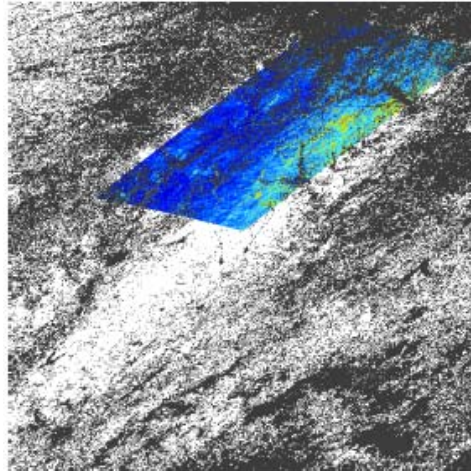
Analysis at 500-m (LAI)

Grassland/ Cereal crops

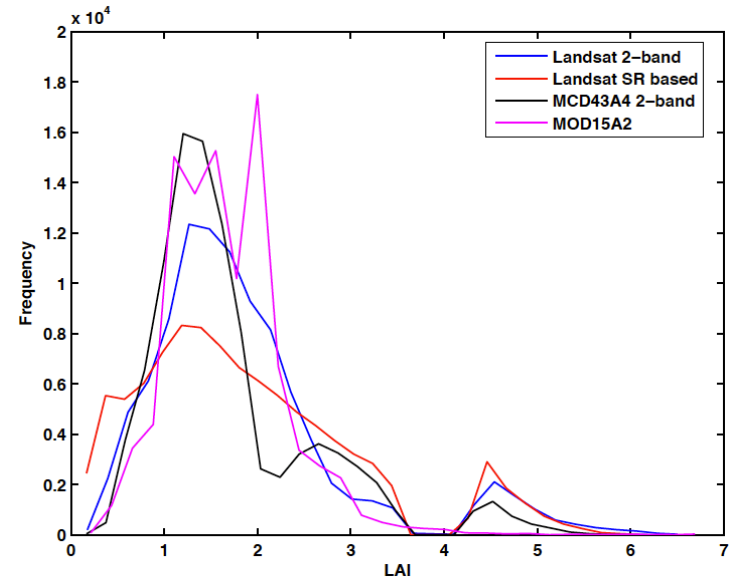
MODIS LAI



Landsat LAI 2-band inversion

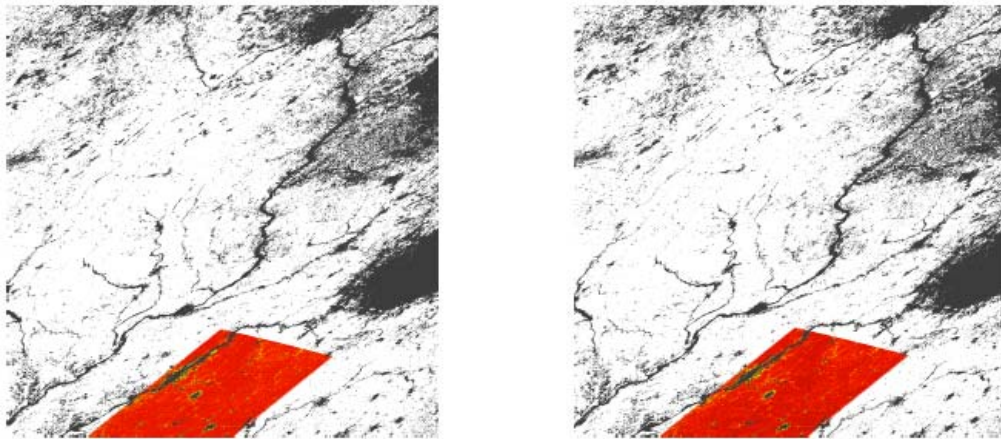


Landsat LAI
Simple Ratio Based



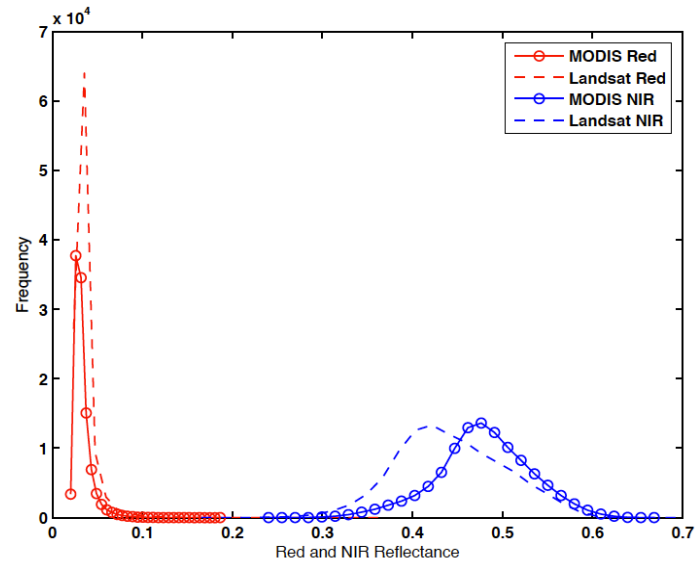
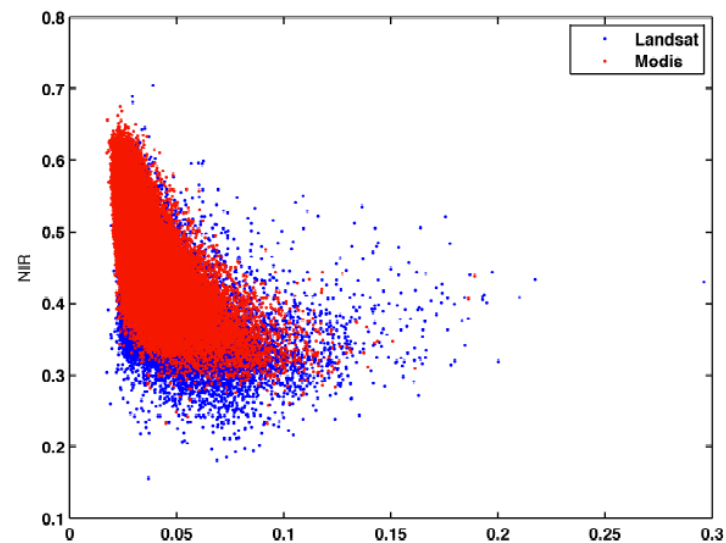
Analysis at 500-m (Surface Reflectance and LAI)

Broadleaf Crops



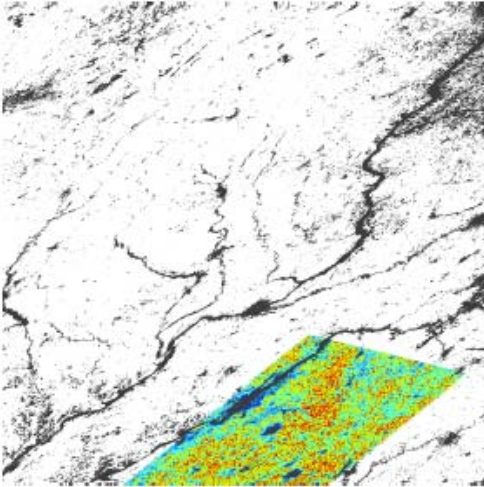
Landsat NDVI

MODIS NDVI

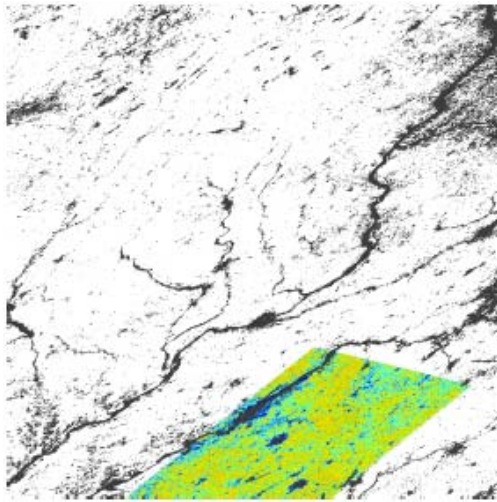
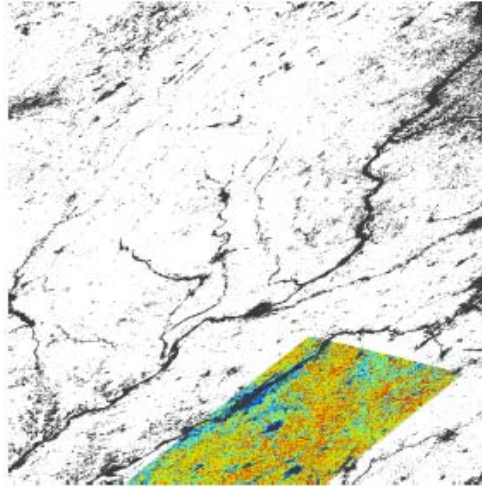


Analysis at 500-m (LAI)

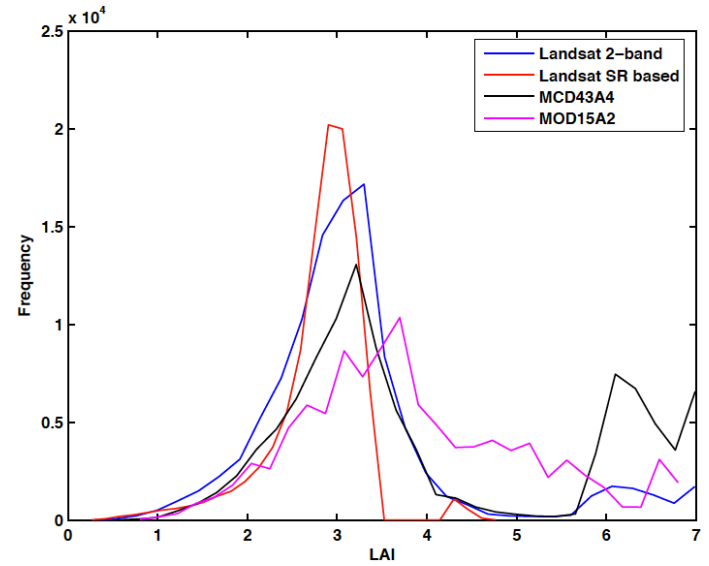
MODIS LAI



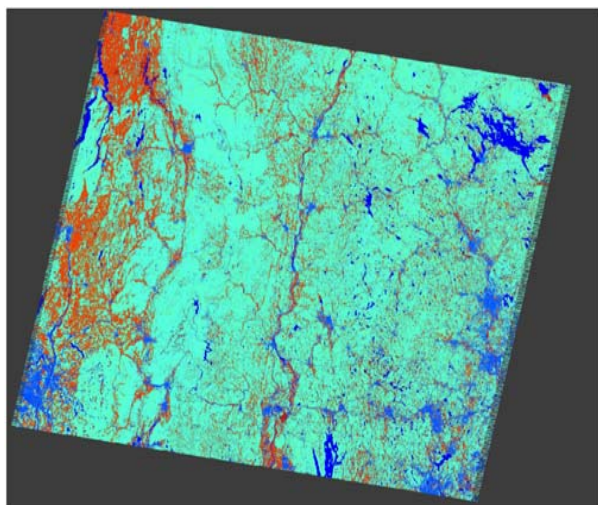
Landsat LAI 2-band inversion



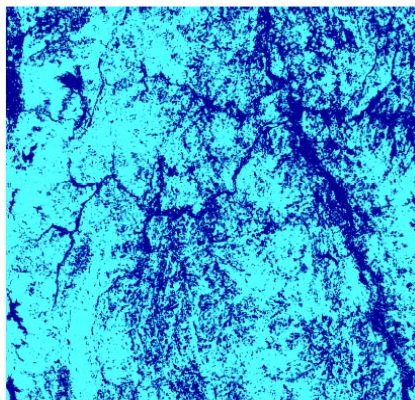
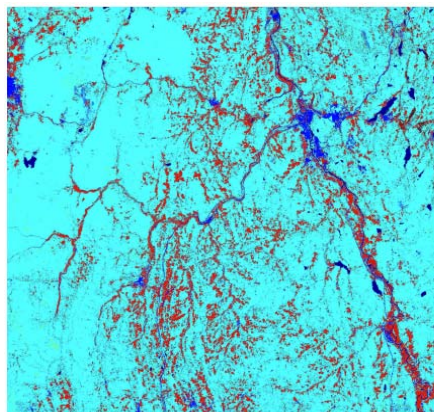
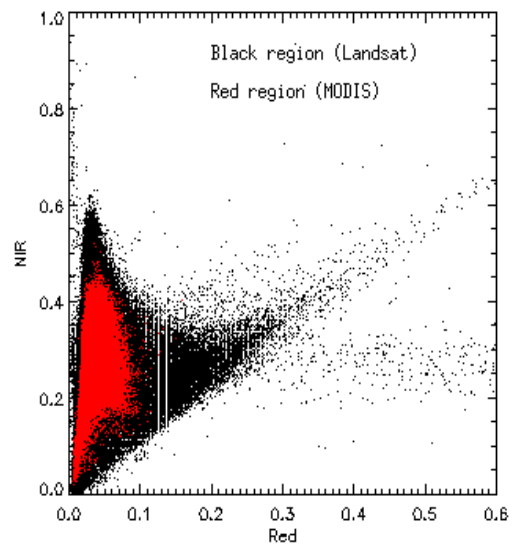
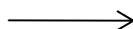
Landsat LAI
Simple Ratio Based



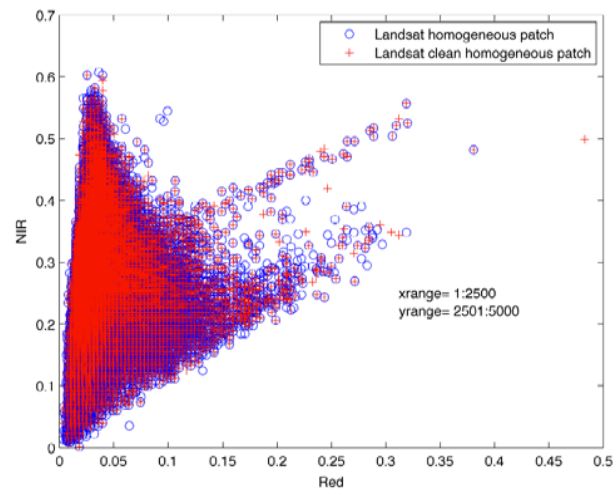
Reflectance Analysis



10 20 30 40 50 60 70 80 90 100
NLCD Landcover



20 40 60 80



Analysis

- Analysis at 500m gives a clear conceptual framework for developing the LUTs – apply simple scaling relations to these LUTs and apply at 30-m;
- NBAR and Landsat reflectances seem to be really consistent at the 500m scale - Landsat reflectances at 30-m averaged to 500m are real averages;
- Downsampling to 30-m should be performed with caution – results can be wrongly interpreted in scaling physical quantities (e.g. reflectances and LAI) – MODIS reflectances scaled to 30-m are simple replications and hence will preserve the same physical nature as in 500-m.

Analysis

- What are the implications in retrieving the LAI at 30-m? – first ever 30-m wall-to-wall leaf density map from Landsat, implications for accurately estimating biomass, high resolution GPP estimation (scaling climate variables of course);
- If reflectance signatures still show the high dynamic range in red reflectances, the LAI retrieved will still be smaller compared to LAI retrieved at any coarse resolution pixel – even after scaling and tuning the LUTs;
- This is the best we can do and developing the basis at 500-m, showing consistency with MODIS and then scaling it back to 30-m is a good feasible approach.

Activities

- LAI maps used by Martha at USDA for irrigation mapping;
- LAI to be created for South East Asia (2005 and 2000) – Atul Jain’s project;
- USGS wants the LAI as a standard higher level product – so with our new computing framework, we can blast through all the scenes and create a first version LAI;
- Current improvement strategies for landcover mapping – use best landcover wherever possible (e.g. NLCD for US);
- Canadian Remote Sensing guys, ISPRA (Italy) and Japan wants the LAI product once released;
- Validation work to start soon – database being built with all available LAI field data;
- Technical paper to be wrapped up by end of this year;
- Next year activity involves refining the product algorithm from validation exercise;
- Atmospheric correction (esp. cloud correction) still to be improved;

Thanks to all of you for providing me all the help and necessary support at every stage in spearheading this project
– This can't be done alone !!